# A novel MR compatible indentation setup to study the etiology of pressure ulcers and related deep tissue injury.

Jules L. Nelissen[1], Willeke A. Traa[2], Larry A. de Graaf[1], Kevin M. Moerman[3], Aart J. Nederveen[3], Cees W. Oomens[2], Klaas Nicolay[1], and Gustav J. Strijkers[1]
[1]*Biomedical NMR, Department of Biomedical Engineering, Eindhoven University of Technology, Eindhoven, Netherlands,* [2]*Soft Tissue Biomechanics and Engineering, Department of Biomedical Engineering, Eindhoven University of Technology, Eindhoven, Netherlands,* [3]*Department of Radiology, Amsterdam Academic Medical Center, Amsterdam, Netherlands*

**Target audience**

(Pre) clinical scientists interested in pressure ulcer research, skeletal muscle damage and musculoskeletal MRI.

**Purpose**

The aim of this study was to design, build, and test a new Magnetic Resonance (MR) compatible indentor for research on the etiology of pressure ulcer related deep tissue injury in the tibialis anterior (TA) skeletal muscle in a Sprague-Dawley (SD) rat model. The indentation setup was built as technical improvement of the previously used setup.[1, 2]

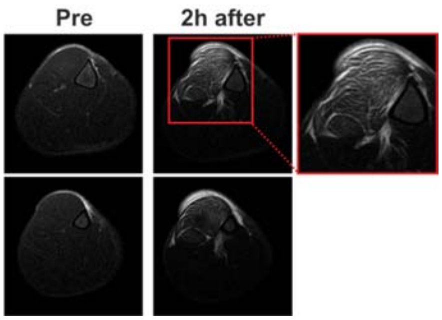


**Fig. 2.** Axial strong T2 weighted images at two different positions in the rat leg, pre and after indentation. Zoom in shows microvasculature.

**Materials & Methods**

<u>*MR compatible indentor:*</u> The indentation device was designed and built to apply sustained mechanical loading to the TA muscle in the rat inside a small animal MR system, leading to deep tissue injury. The device, shown in **Fig. 1 A**, consists of a holder with a rotatable half arch, on which the indentor can be moved to allow flexible positioning. The indentor has a cylindrical shape (diameter 3 mm, length 36.5 mm) with a rounded head, filled with 1g/L $CuSO_4$, to provide MR detection (**Fig. 1 A , B**).

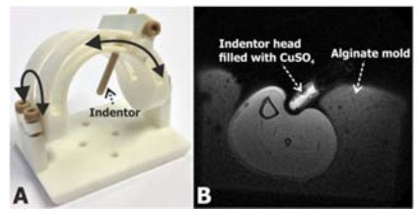


**Fig. 1. A**: MR compatible indentation device. Arrows indicate the flexible positioning options of the indentor. **B**: 2D UTE of TA muscle under loading. Alginate mold and indentor are indicated with arrows.

<u>*Rat model:*</u> 7-week-old SD rats (♀, 162-220 gram, n=7) were used. The right leg of the rat was shaved and placed in a plastic profile filled with alginate molding substance for firm fixation, while keeping the TA muscle accessible for indentation. Alginate has the additional advantage that it can be visualized using ultra-short echo time (UTE) MRI (**Fig. 1 B**). The rat was placed in the MR compatible indentation setup. Indentation of the TA muscle, for a period of 2 hours, took place inside the MR scanner.

<u>*In vivo MRI:*</u> A Bruker 7.0T small animal MRI scanner was used with a 2 cm diameter receive surface coil, placed on top of the TA muscle inside the indentation device, in combination with a 86 mm excitation volume coil. Skeletal muscle injury and physiological changes were assessed with T2 mapping (Spin-Echo, 20 slices, FOV = 2.5 x 2.5 $cm^2$, MTX = 256 x 256, TE = 6.95 – 180.7 ms, 26 echos, TR = 4 s, fat suppression), strong T2 weighted (Spin-Echo, 20 slices, FOV = 2.5 x 2.5 $cm^2$, MTX = 256 x 256, 10 summed echos, TE-effective = 70 ms, TR = 2 s), and Time-Of-Flight (TOF) angiography (FLASH, 120 slices, FOV = 4 x 4 $cm^2$, MTX = 256 x 256, TE = 3.8 ms, TR = 12 ms) protocols. Anatomical and geometrical information was assessed with T1-weighted MRI. All measurements were performed pre, during and up to 2 h after indentation. During the MRI scans and indentation isoflurane (1-2%) was used as anesthetic.

<u>*Data analysis:*</u> Quantitative T2 maps were obtained by fitting the MR signal pixel wise. Pixels with $R^2 < 0.7$ and SNR < 4 were excluded. Region of interest based T2 analysis on the TA muscle pre and 1h after indentation was performed in 4 slices around the position of indentation. The TOF angiograms were processed by visualizing maximum intensity projections (MIP).

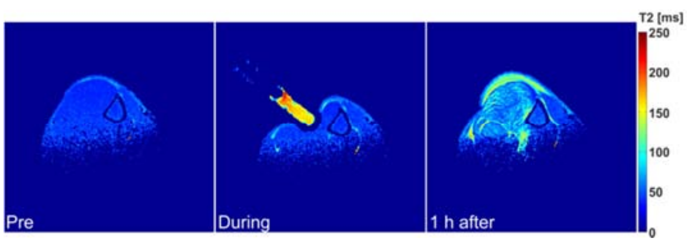


**Fig. 3.** Quantitative T2 maps of TA muscle pre, during and after indentation.

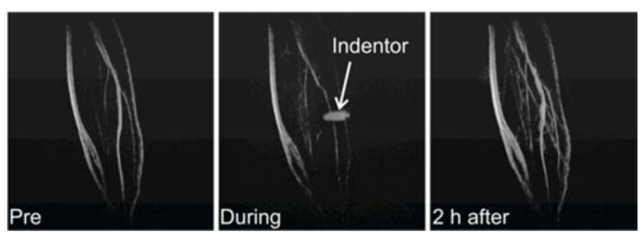


**Fig. 4.** MIP angiography images of rat leg pre, during and after indentation.

**Results and Discussion**

**Fig. 2** shows two axial strong T2 weighted slices at two different positions in the rat leg, pre and after 2h of deformation. Hyperenhancement due to the formation of edema is already visible in the images within 10 min after load removal, with intensity increasing over time. The hyperenhancement resembles the structure of the microvasculature, which has been implicated in the development of deep tissue injury before.[3] To our knowledge the visualization of the microvasculature has never been visualized in relation to deep tissue injury before. In **Fig. 3** quantitative T2 maps pre, during, and after indentation of the TA muscle are shown. Increased T2 values compared to pre and during indentation were observed in the T2 map after 1h of indentation. The T2 enhancement pattern showed the same capillary bed structure, as in Fig. 2. In addition, elevated T2 values were detected between skin and muscle, indicating the formation of edema. No T2 increase was observed during indentation. ROI T2 analysis of the TA muscle pre and 1h after indentation revealed a significant (paired t-test, $p<0.001$) increase in T2, from 38.2 ± 4.8 ms pre to 60.0 ± 11.6 ms after indentation. **Fig. 4** shows MIP of the blood vessels in the rat leg pre, during and 2h after indentation. Application of a load to the TA muscle with the indentor resulted in collapse of a main supplying vessel, whereas several smaller vessels became visible, which could indicate a compensatory mechanism in collateral vessels to account for loss of blood supply. After load release more small vessels became visible, indicative for a hyperemic effect.

**Conclusion**

A new Magnetic Resonance (MR) compatible indentor was successfully designed, built, and tested. After application of the indentor to TA muscle inside the MRI scanner, increased contrast was observed on T2 weighted scans and T2 maps which can be related to the development of deep tissue injury. Angiography revealed a collapse of larger blood supplying vessels and a hyperemic effect after load release. We expect that the use of this novel device will provide new insights in the etiology of pressure ulcer related deep tissue injury.

**Acknowledgement**

This research was supported by the Dutch Technology Foundation STW, the Applied Science Division of NWO, and the Technology Program of the Ministry of Economic Affairs

**References** 1) Loerakker *et al.* J. Appl. Physiol. 2011 2) Stekelenburg *et al.* Med. Eng. Phys, 2006 3) Linder-Ganz and Gefen *et al.* Ann BioMed Eng, 2007